

## CHAPTER 3

### QUANTITATIVE ANALYSIS OF ATOM-PROBE DATA FOR STUDIES

#### OF CONTINUOUS PHASE CHANGES:

#### A FOURIER TRANSFORM METHOD

### 3.1 Introduction to Phase Separation Studies

#### 3.1.1 The Suitability of the Atom-Probe

Spinodal phase separation in metallic systems is characterised by continuous increase in amplitude of a compositional modulation wave of periodicity in the range 5-20nm (e.g. Hilliard 1970). The general suitability of the atom-probe for studies of these modulations has already been demonstrated by Watts and Ralph 1977, 1978. Only semi-quantitative numerical analyses could be applied by Watts and Ralph to growth of compositional excursions, however, because data chains were too short for the accurate spectral analyses required for tests of the diffusion equation given in Chapter 2 above. This restriction upon statistical confidence has been removed in the present study by extension of effective data chain length to 40-60nm per chain. Primarily, this ten-fold improvement has been achieved by implementation of computer-controlled methods of data collection.

As a result of chain extension, methods of analysis to extract spectral components from data are required. This chapter develops one such new method based upon Fourier transform filtering. Instrumentation and experimental requirements for data collection are not considered in this account since most pertinent factors are discussed by Watts and Ralph 1978. More recent changes in instrumentation (e.g. fast pulse technology (Waugh 1980) and updating



of computer controlled data collection) are discussed in Appendix A.

### 3.1.2 The Nature of Atom-probe Data Chains

The data from atom-probe studies appear as a chain of discrete ion events. These events must be combined to represent the physical compositional wave as a plot of composition against distance probed into the specimen. The means by which the data are grouped, and hence the possible routes of numerical analysis of the composition profile, depend upon the model of the time series which is used to describe the process of field evaporation.

#### 3.1.2i Markov Process

A specific description of atom-probe data as a Markov Chain was suggested by Johnson and Klotz 1971. By definition this requires that the state of the system  $X_t$  is characterised by a knowledge of  $X_{t-1}$  only and is independent of preceding events (Jenkins and Watts 1968). In terms of atom probe data this demands that  $X_{t-1}$  provide information concerning lattice structure. Johnson and Klotz justified their approach by considering adjacent atoms in the data chain to be nearest neighbours in the specimen. Even with a projected probe hole of single atom diameter, as assumed by Johnson and Klotz, the nearest neighbour approximation may be invalidated by atomic migration. For studies of phase changes a probe hole encompassing 50-100 atoms is required for compositional analysis (Watts and Ralph 1978) and in this case the nearest neighbour model certainly fails because atoms under occurrence of a selected chemical species directly as a function of total ion count (probing distance) or remaining species. Using small steps of 1-20 ions through the data chain emphasizes abrupt changes



the probe hole may be expected to evaporate in near-random order.

### 3.1.2ii Random evaporation process

A general discrete time series analysis based upon random evaporation from material under the probe hole has been suggested by Watts and Ralph 1978. In their model the data chain, assumed for simplicity to sample a binary system, is regarded as a series of A atoms (minor species) spaced by B atoms. Using data for Ni-12at.%Ti alloy Watts and Ralph justified their method by demonstrating that the calculated distribution of A (Ti) atoms approximated that predicted by the binomial theorem. This approach is certainly more realistic than the Markov treatment and the assumption of random evaporation is taken as the basis of the present analytical study. Some possible inadequacies of this assumption are discussed in section 3.6.

### 3.1.3 Composition Profiles

All methods for conversion of time series of A events into composition profiles (see section 3.1.3 below) seek to define the specimen composition at predetermined sampling intervals by expressing the relative frequency of occurrence of A events in terms of total ion count i.e. probing distance. Three basic types of composition profile may be distinguished.

#### 3.1.3i Step profile

The step profile (e.g. Goodman, Brenner and Low 1973) plots the occurrence of a selected chemical species directly as a function of total ion count (probing distance) or remaining species. Using small steps of 1-20 ions through the data chain emphasises abrupt changes



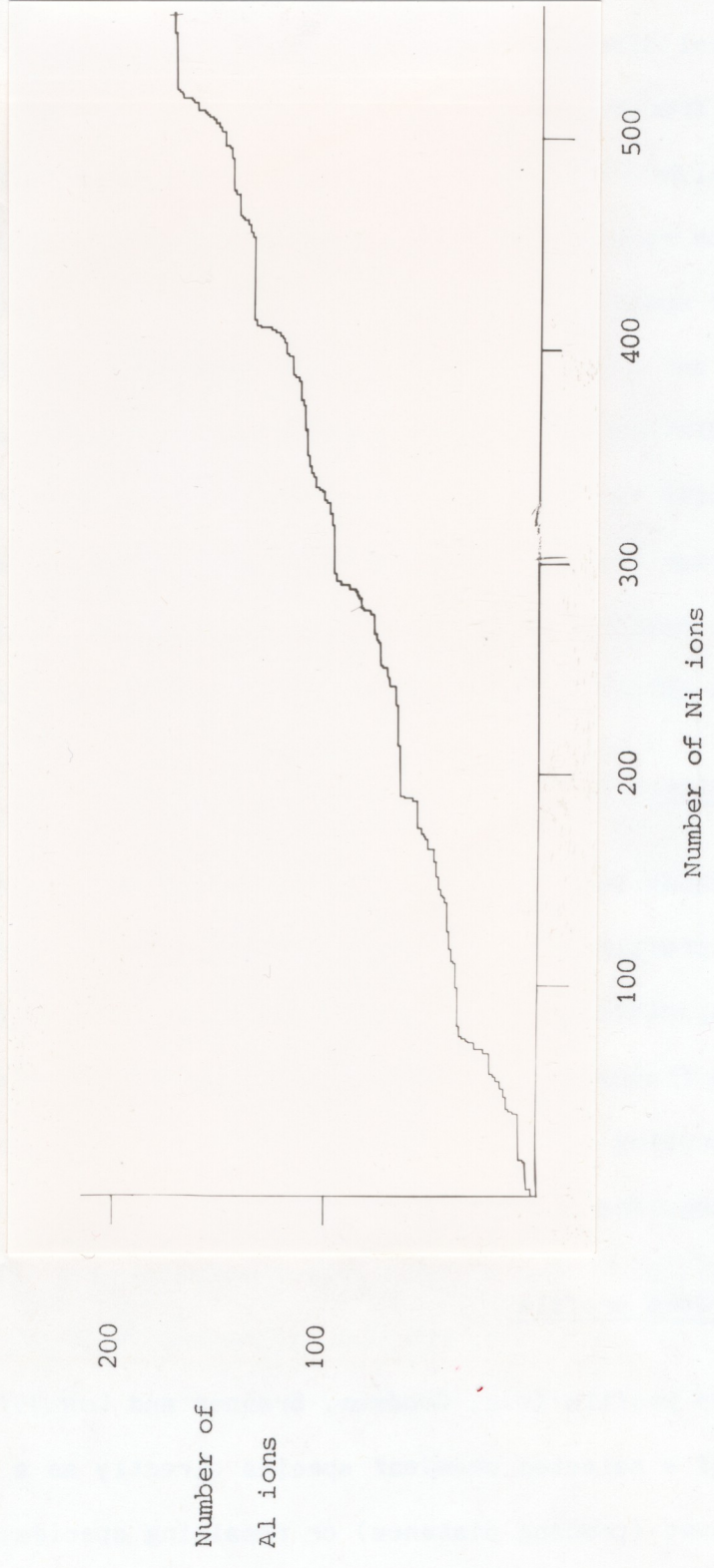


Figure 3.1 Step profile for a  $\langle 110 \rangle$  probing sequence in a  $\text{Ni}_3\text{Al}$  single crystal.



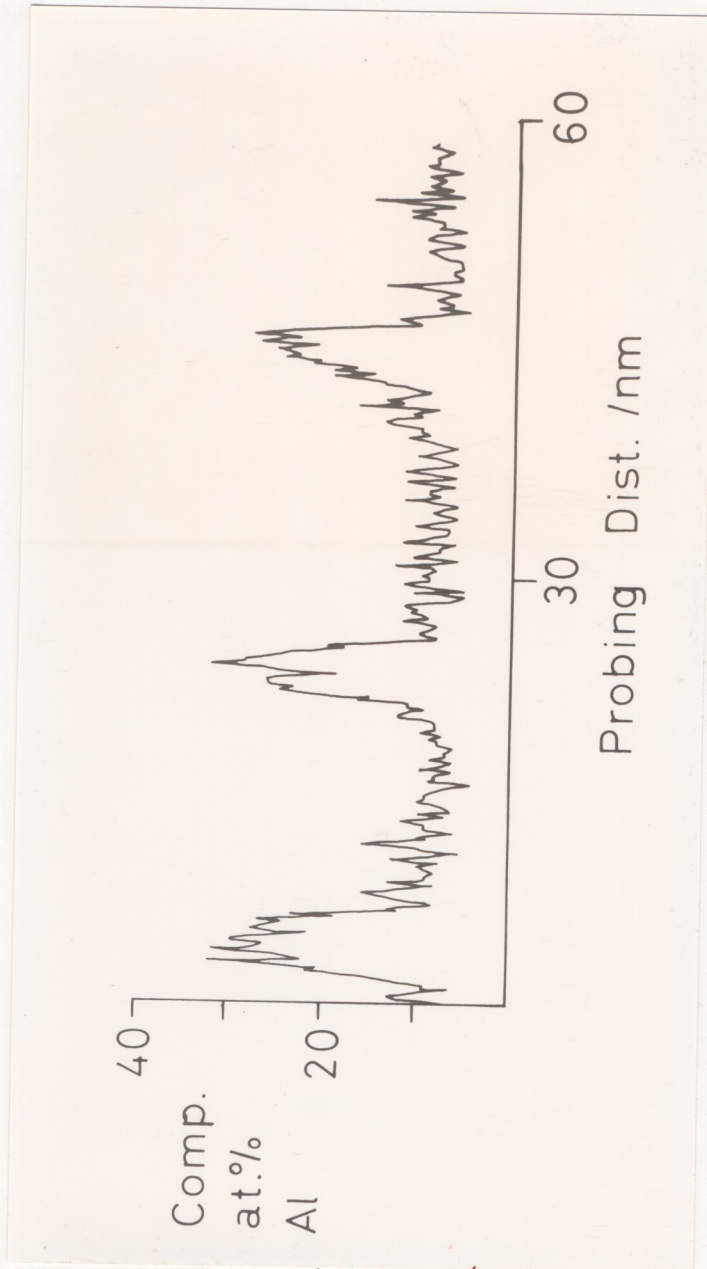


Figure 3.2 Simple grouping profile (200 ions per point) for Ni-16.1at%Al alloy aged for 50 hours at 625°C.

Figure 3.1 Step profile for a <110> probing sequence in a Ni<sub>3</sub>Al single crystal.



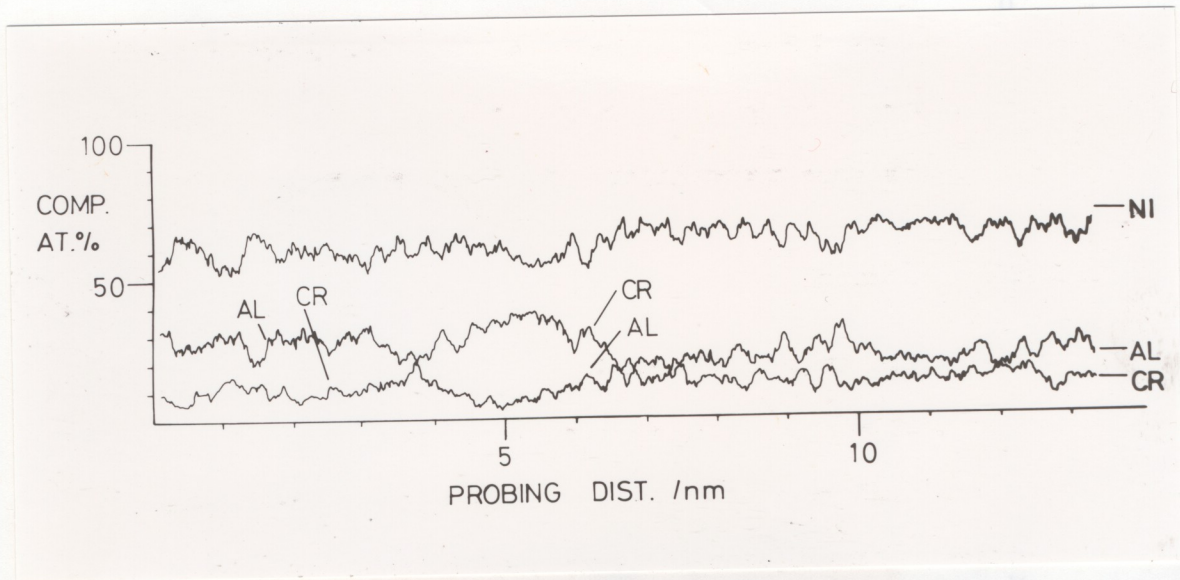


Figure 3.3 Running mean plot of data from an analysis of Ni-20.0at%Cr-14.0at%Al alloy aged for 5 minutes at 620°C (two-phase).

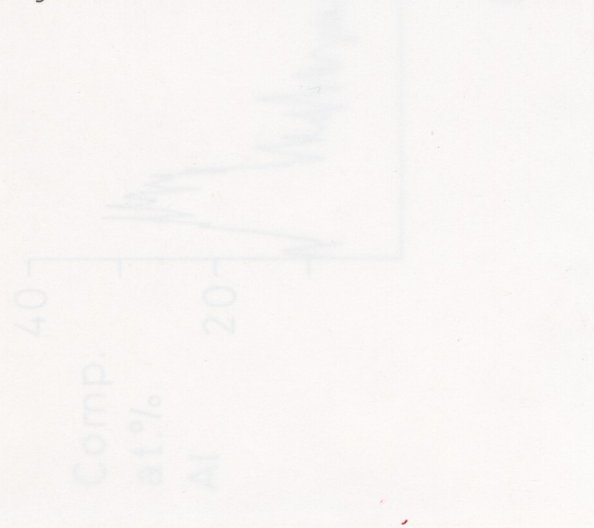


Figure 3.2 Simple grouping profile (200 nm)



in composition between adjacent planes and composition excursions of short periodicities. This technique is suitable for studies of order-disorder reactions (e.g. Taunt and Ralph 1974), interface development and various forms of segregation (e.g. Southon and Southon and Waugh/1977). The method is illustrated in figure 3.1 which shows part of a step profile for a  $\langle 110 \rangle$  probing sequence in an  $\text{Ni}_3\text{Al}$  single crystal. Adjacent ordered superlattice planes have compositions of 100%Ni and 50%Ni + 50%Al.

### 3.1.3ii Simple Grouping

For longer data strings the chain may be divided into larger sub-units, say 200-1000 ions. Assuming that each unit represents a small volume of material of constant composition within the sample, this gives a profile of composition in atom% versus ion count. With suitable correction in sub-unit size for changes in tip radius i.e. changes in the number of ions collected per atomic plane (section 3.4.ii below) the plot corresponds to a composition against distance profile. Figure 3.2 shows such a plot for Ni-14.1at.%Al alloy aged for 50 hours at  $625^\circ\text{C}$  (probing direction  $\langle 110 \rangle$ , 200 ions per point).

This method sacrifices information contained within each sub-unit, but it is suitable for studies of long range effects such as clustering phenomena.

### 3.1.3iii Running means

The running mean is also used for study of long range phenomena. In its simplest form the method again defines a small chain sub-unit,  $t$ , of 10-20 ions, and composition values as at% are then plotted over  $n$  terms at intervals of  $t$  (e.g. Yule and Kendall 1968). Figure 3.3 shows data from an analysis of two-phase Ni-20.0at.%Cr-14.0at.%Al



alloy (Chapter 5) plotted in running mean form.

This simple form, however, still rejects information within sub-units. A statistical running mean was therefore proposed by Watts and Ralph 1978. Where  $U$  denotes the number of B atoms separating adjacent A atoms, the  $n$ th term of  $U$  in the time series is replaced by an average over  $2t+1$  values.

The disadvantages of running mean methods are conversion of composition steps to gradients and loss of high frequency oscillations in the original composition data.

#### 3.1.4 Methods of Analysis

Once a suitable composition profile has been produced it may be subjected to some general time-series analysis or trend removal (e.g. correlation coefficient studies or Fourier transform methods) in order to follow the development of the component wavelengths.

For studies of continuous changes Fourier transform techniques are the most appropriate because results may be compared directly with predictions of transition theories which are expressed as Fourier solutions (Chapter 2). In addition Fourier analysis of composition data should produce results which are comparable with diffraction patterns such as those of TEM or X-ray work. This interrelation of diffraction studies and modulated microstructure has been clearly demonstrated by de Fontaine (1966) using an electronic analogue.

The present study is therefore devoted to two topics: i) construction of a composition profile suitable for Fourier transform and ii) development of a method of Fourier transformation by which to



assess as accurately as possible the relative amplitudes of dominant Fourier components. Possible extensions of the method to study of other phase changes are discussed in section 3.6.

### 3.2 Formal Fourier Transform Theory

#### 3.2.1 General Fourier Transform (FT)

##### 3.2.1.1 Theory

The Fourier Transform,  $F(\omega)$ , (Champeney 1973; Brigham 1974; Bracewell 1978) expresses an aperiodic function,  $f(t)$ , in terms of a continuous range of frequencies,  $\omega$ :

$$E(\omega) = \frac{1}{(2\pi)^{1/2}} \int_{-\infty}^{+\infty} f(t) \exp(-i\omega t) dt \quad \dots E3.1$$

In order to assess the overall contributions of specific frequencies (wavenumbers) this equation may be rewritten in terms of the coefficients of the cosine and sine terms which comprise the waveform.

Thus:

$$A_n(\omega) = \frac{1}{\pi} \int_{-\infty}^{+\infty} f(t) \cos(\omega t) dt \quad \dots E3.2$$

$$B_n(\omega) = \frac{1}{\pi} \int_{-\infty}^{+\infty} f(t) \sin(\omega t) dt \quad \dots E3.3$$

where  $A_n$  and  $B_n$  represent the cosine and sine coefficients respectively.

Two specific functions represented in symbolic notation are referenced in the present work. These are the rectangular function



$\Pi(t)$  (a sampling window of unit height and base) and the infinite impulse train  $\text{III}(t)$  which corresponds to discrete data sampling at a fixed interval. Both functions and their Fourier transforms are illustrated in Appendix C.1

### 3.2.2 Discrete Fourier Transform (DFT)

#### 3.2.2i Theory

DFT operates where values of a function or transform are available only at discrete intervals. Experimental data are an example of a discrete input stream.

Expressions for DFT are essentially very similar to general FT solutions, but with integrations replaced by summation over the appropriate range of variable. For example the DFT itself is:

$$F(v) = \frac{1}{N} \sum_{\tau=0}^{N-1} f(\tau) \exp(-2\pi i v \tau / N) \quad \dots E3.4$$

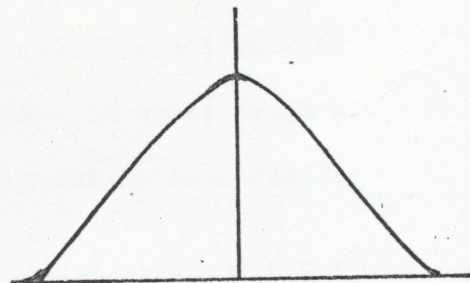
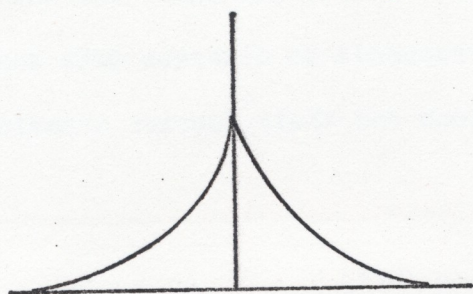
Beginning with data sampling of a function using the infinite impulse train  $\text{III}(t)$  Appendix C.2 illustrates the series of steps which leads to the Fourier transform of experimental data.

The CONVOLUTION THEOREM (e.g. Bracewell 1978) and its inverse, the PRODUCT THEOREM, are referenced particularly in the following text. These theorems state that for two sequences (DFT) (or functions (FT)) convolved in the data domain the transforms are multiplied in the transform domain and vice versa. Stated formally the convolution theorem is:



Function

Transform



$\times$

$*$

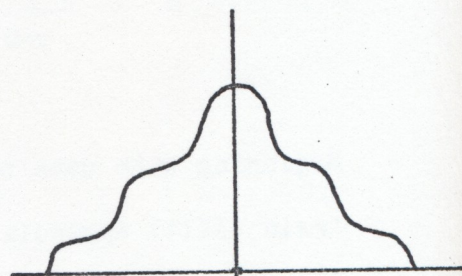
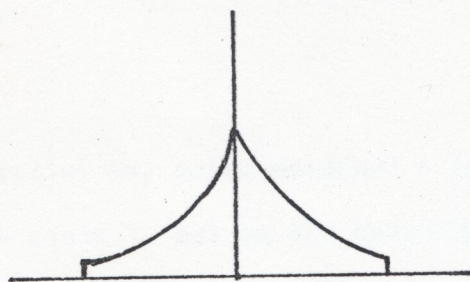
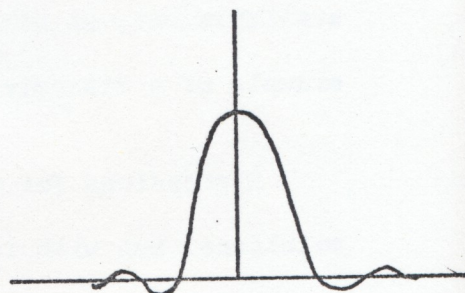
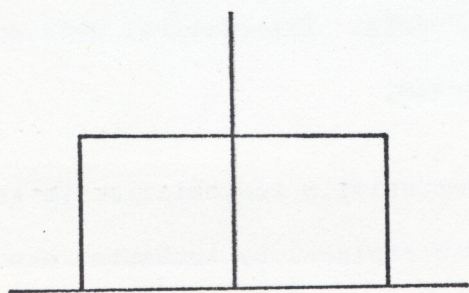


Figure 3.4 Result of truncation using a rectangular function



$$f(t) * g(t) = F(\omega) G(\omega)$$

....E3.5

### 3.2.2ii Calculation

Methods of calculation are summarised in the references. By far the most popular is an algorithm due to Cooley and Tukey (see e.g. Bracewell 1978), known as the Fast Fourier Transform (FFT). This is somewhat less accurate than other methods, but computation is much faster.

In terms of limitations imposed upon input experimental data, all methods should ideally operate upon an oscillating and noiseless physical waveform.

### 3.2.2iii Errors

Major errors in DFT may arise from inappropriate data truncation or sampling.

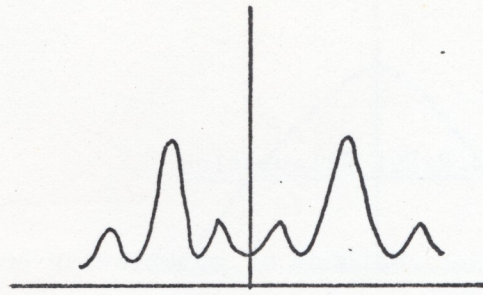
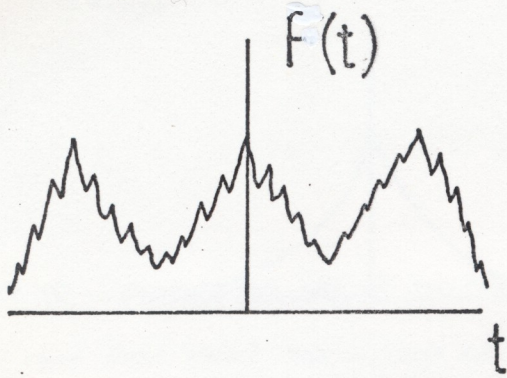
#### Truncation

Experimental data chains must be regarded as sections selected from a much longer chain using a rectangular data window  $\Pi(t)$ . The result of selection seen in the transform domain (product theorem) is convolution of the true DFT with a sinc function ( $\sin\pi x/\pi x$ ). This is illustrated in figure 3.4. Thus the original DFT becomes smoothed and some falsification of higher frequencies may arise from "leakage error" associated with higher terms of the sinc function (e.g. Bracewell 1978). These inherent errors are unavoidable, but may be reduced for low wavenumbers by increasing data chain length.



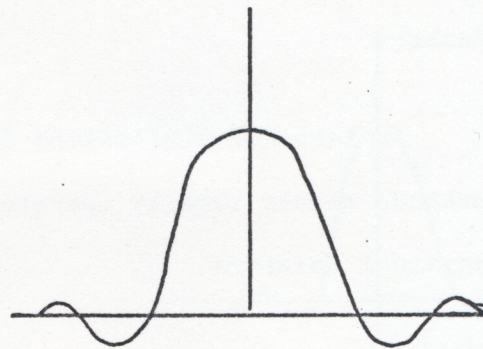
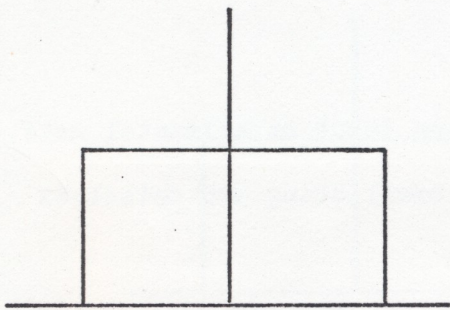
Function

Transform



\*

x



↓

↓

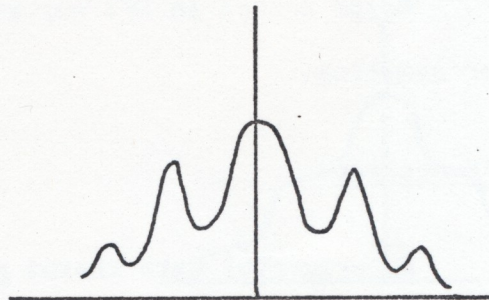
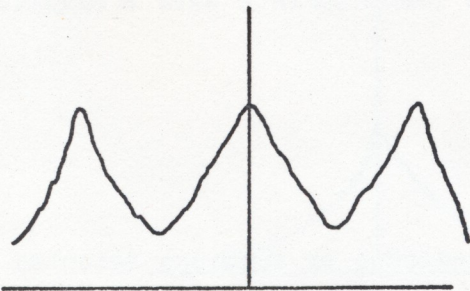


Figure 3.5 Result in the transform domain of performing a running mean in the data domain.



the For the Cooley-Tukey algorithm  $2^N$  data values are required.

"Packing" of domains to satisfy this requirement may introduce further error. If zero values are imposed upon a chain of non-zero-mean data a step is produced in the input stream and rough structure in the net transform. Thus packing must employ dummy variables.

### Sampling

Essentially the data sampling interval must be selected such that the wave of highest frequency is sampled at least twice per wavelength (critical sampling). Undersampling generally results in loss of fine detail. Additionally "aliasing" may occur, high frequencies "impersonating" lower frequencies (e.g. Bracewell 1978)

For low wavenumbers transforms may also be inaccurate if few complete long wavelengths are sampled.

### 3.3 A Composition Profile for Fourier Transform: Introduction of a New Analysis Route

Of the three methods described in section 3.1.3 above only simple grouping is appropriate for Fourier transform. The step profile cannot be used because it is non-oscillatory, being possessed of a trend derived from the form of construction. It is also very noisy.

The running mean is undesirable because the transform contains terms from the smoothing function. In Fourier terminology the compositional data are convolved with a rectangular sampling function  $\Pi(x)$ , of width  $(2t+1)$  terms, in the data domain. Thus the transform is multiplied (convolution theorem) by  $\text{sinc}(x)$ . This is illustrated in figure 3.5. In principle the  $\text{sinc}(x)$  terms may be recovered from



the net transform.

The following Fourier transform treatment is therefore developed for a composition profile of simple grouping type. The spatial information which is lost within grouping units may be recovered from the original data by the alternative methods described in the present section.

### 3.4 The <sup>New</sup> Fourier Transform Route.

#### 3.4.1 Construction of the Composition Profile.

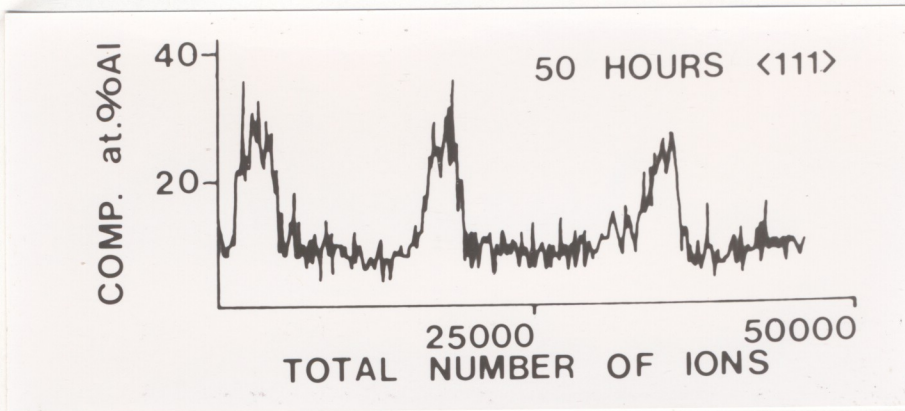
##### 3.4.1i Sampling

Two factors must be considered in selection of sampling size. Small units tend to introduce noise into the profile and cause loss of significance in the transform. Undersampling leads to aliasing in the transform (section 3.2 above) and also general loss of accuracy by reduction in available data values. The optimum solution to balance these factors retains the maximum number of compositional values,  $C_n$ , while giving acceptably small background variance in the transform (section 3.4.3 below). An approximate optimum solution may be obtained by trial and error, selecting a unit size for the composition profile and observing the transform.

The physical significance of each sub-unit,  $m$ , should also be considered. The separation of components in the transform domain is reciprocally related to the distance between compositional determinations,  $C_n$ , in the sampling domain. Thus if samples contain some multiple of the number of ions detected per atomic plane, the Fourier wavenumbers are inversely related to the interplanar spacing.



a)



b)

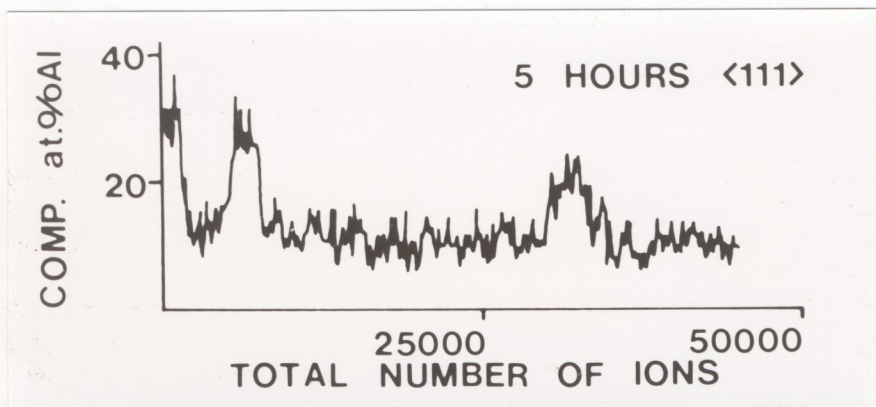


Figure 3.6 Optimized simple grouping profiles (150 ions per point) for Ni-14.1 at%Al alloy aged for a) 5 hours and b) 50 hours at 625°C.



If it is necessary to suppress composition modulations which arise from planar stacking sequences, this may be achieved by selection of a unit size appropriate to the lattice repeat (or some multiple thereof).

Several problems are associated with the grouping. First, the ion count per plane varies as a function of probing voltage and also as a function of probing direction. The former may be counteracted by adjustment of unit size on a sliding scale calibrated using an ordered single crystal (e.g.  $L1_2$ ,  $Ni_3Al$ ). The effect of probing direction is measurable using the same single crystal and may be estimated from crystallographic considerations.

Second, where compositional modulations are present, and particularly in cases of lattice ordering, the exact profile produced may be extremely sensitive to starting position along the data chain. Thus it is recommended that a step profile of each data chain be examined before chain sub-division. For cases where the composition profile,  $C_n$ , is origin-dependent, step analyses will detect plane-to-plane compositional discontinuities and provide an origin location (figure 3.1).

For situations where little origin-dependence is seen, minor effects may be counteracted, if required, by an averaging procedure. Three composition plots are derived starting at i) an arbitrary origin 0, ii) a distance  $m/3$  from the origin and iii)  $2m/3$  from the origin, where  $m$  is the sub-unit size. All three are transformed and the results summed and averaged as detailed below in section 3.4.2iii.

Two examples of optimised traces are shown in figure 3.6.



Figure 3.6b replots the data used for figure 3.2 in optimized form for comparative purposes. Figure 3.6a shows data from another specimen of the same alloy aged for 5 hours at 625°C. In all cases the unit size is 150 ions for a tip at 11.6 kV and <111> probing direction. This choice describes two lattice planes. The equivalent grouping for <110> would suppress the two-layer lattice repeat of  $L1_2 Ni_3Al$ . Thus <110> transforms may be compared directly with <111> data which shows no lattice-related compositional modulations.

#### 3.4.1ii Truncation.

The profile thus far oscillates about a positive mean and is of non-standard length for DFFT. Calculation of the mean and subtraction of this from each separate data value gives an oscillating series about zero. Dummy variables of zero may then be used to extend the reduced profile,  $C_n^R$ , to the required length.

#### 3.4.2 Transform Steps

##### 3.4.2i Initial transform

The stages of Fourier transform are illustrated in figure 3.7. Once the reduced profile  $C_n^R$  has been transformed, sampling errors are still present at the low frequency end of the Fourier spectrum because insufficient long wavelengths are present in the data chain for accurate analysis. A correction may be applied for this by subtracting from the original data the effects of the invalid low frequencies. Thus the significance of terms of interest in spinodal studies (0.8-20.0nm) is increased.



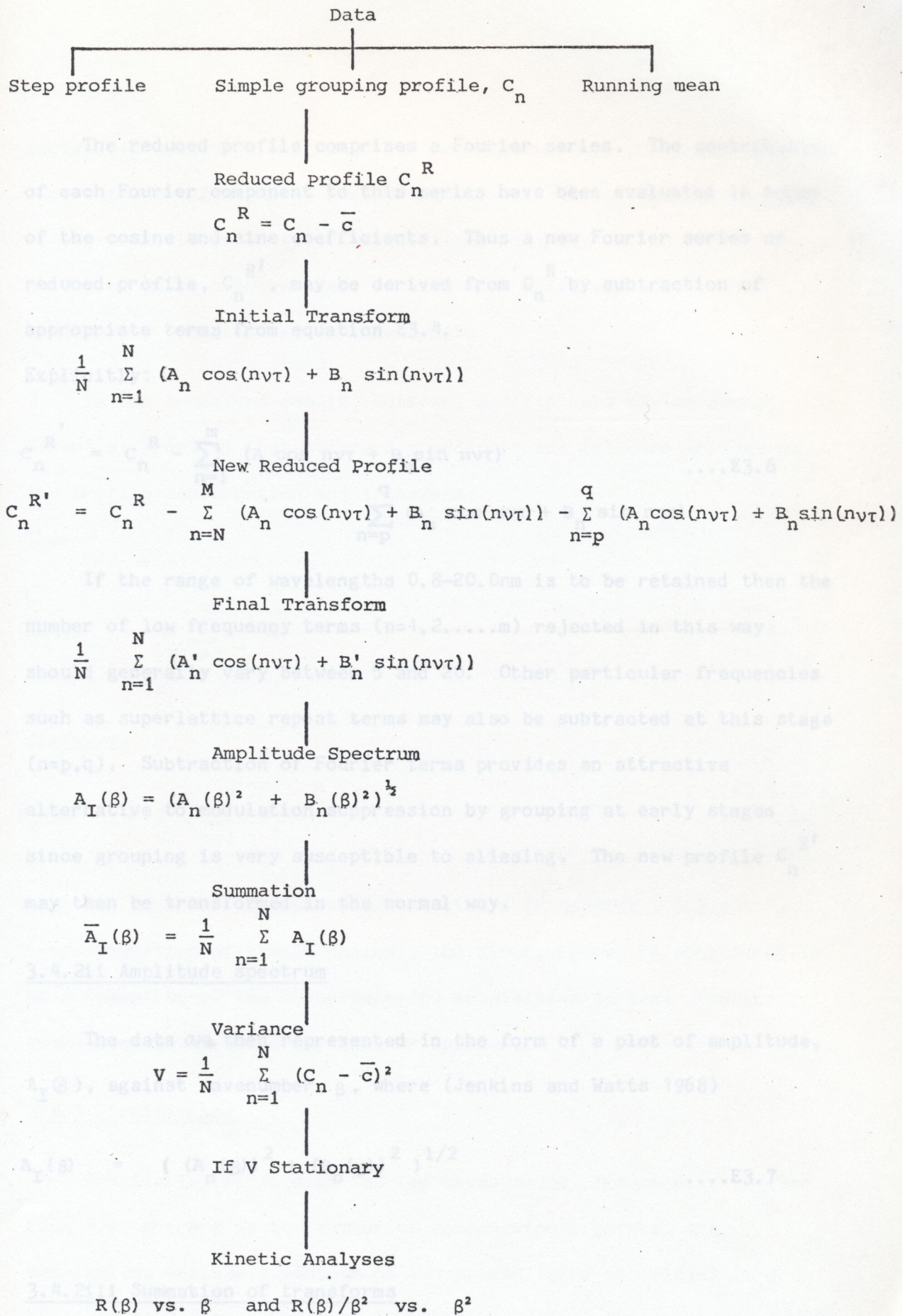


Figure 3.7 Stages of Fourier Transformation



The reduced profile comprises a Fourier series. The contribution of each Fourier component to this series have been evaluated in terms of the cosine and sine coefficients. Thus a new Fourier series or reduced profile,  $C_n^{R'}$ , may be derived from  $C_n^R$  by subtraction of appropriate terms from equation E3.4.

Explicitly:

$$C_n^{R'} = C_n^R - \sum_{n=1}^m (A_n \cos n\tau + B_n \sin n\tau) - \sum_{n=p}^q (A_n \cos n\tau + B_n \sin n\tau) \quad \dots E3.6$$

If the range of wavelengths 0.8-20.0nm is to be retained then the number of low frequency terms ( $n=1,2,\dots,m$ ) rejected in this way should generally vary between 5 and 20. Other particular frequencies such as superlattice repeat terms may also be subtracted at this stage ( $n=p,q$ ). Subtraction of Fourier terms provides an attractive alternative to modulation suppression by grouping at early stages since grouping is very susceptible to aliasing. The new profile  $C_n^{R'}$  may then be transformed in the normal way.

### 3.4.2ii Amplitude spectrum

The data are then represented in the form of a plot of amplitude,  $A_I(\beta)$ , against wavenumber,  $\beta$ , where (Jenkins and Watts 1968)

$$A_I(\beta) = ( (A_n(\beta))^2 + (B_n(\beta))^2 )^{1/2} \quad \dots E3.7$$

### 3.4.2iii Summation of transforms

Where more than one data chain is available to characterise the microstructure of each heat treatment some method of combining



individual chains to represent the net structure is required. Direct concatenation of adjacent chains (same specimen) in the data domain requires knowledge of the distance separating the chains and/or the change of phase between them. Chains from different specimens cannot be directly concatenated in this domain.

In the transform domain, however, coefficients may be summed directly, provided that standard procedures are followed throughout for profile construction and transform.

Thus

$$\bar{A}_I(\beta) = \frac{1}{N} \sum_{n=1}^N A_I(\beta) \quad \dots E3.8$$

Similarly

$$\bar{B}_I(\beta) = \frac{1}{N} \sum_{n=1}^N B_I(\beta) \quad \dots E3.9$$

For the averaging procedure mentioned in section 3.4.1i, (representation of single chains), the structure may be considered to be a summation of the three separate composition series. Fourier summations given above may then be applied.

### 3.4.3 Significance

Considering first high Fourier wavenumbers, frequencies greater than  $N/2$ , where  $N$  is the number of compositional points, are meaningless because a minimum of two points (plus an origin) is required to define a waveform (critical sampling, see section 3.2.2iii above). In practical terms this region of the spectrum, ( $\beta < N/2$ ), may also be complicated by superlattice components. Thus for



clustering studies frequencies in the range  $N/4$  and above should be regarded with caution.

At the low frequency end the first few Fourier components are rendered inaccessible by virtue of the numerical exclusion employed in the transform procedure (section 3.4.2i above).

This, however, leaves a large range of terms which may be examined. Consider a data chain of 75,000 ions corresponding to 1000 atomic planes or  $\sim 200\text{nm}$  probing distance. A range of frequencies  $\beta = 0.5 \times 10^8$  to  $\beta = 2.5 \times 10^8$  corresponds to wavelengths 20.0-0.4nm. This more than covers the range of modulations found in most metallic spinodal structures.

For these remaining terms the amplitude spectrum may be expected to show distinct peaks at dominant periodicities. Statistical significance of the major frequencies may be tested in a variety of ways (e.g. Yule and Kendall 1968). Variance was selected for the present study. As frequency terms are rejected from extremities of the spectrum the overall variance cannot typify specific central wavenumber regions. Thus local background variance calculations should be performed for each region of interest.

The variance,  $V$ , of data is given by

$$V = \frac{1}{N} \sum_{n=1}^N (A_n - \bar{A})^2 = \sigma^2 \quad \dots E3.10$$

where  $\bar{A}$  = arithmetic mean amplitude

$\sigma$  = standard deviation

For a profile showing strongly dominant periodicities superposed upon



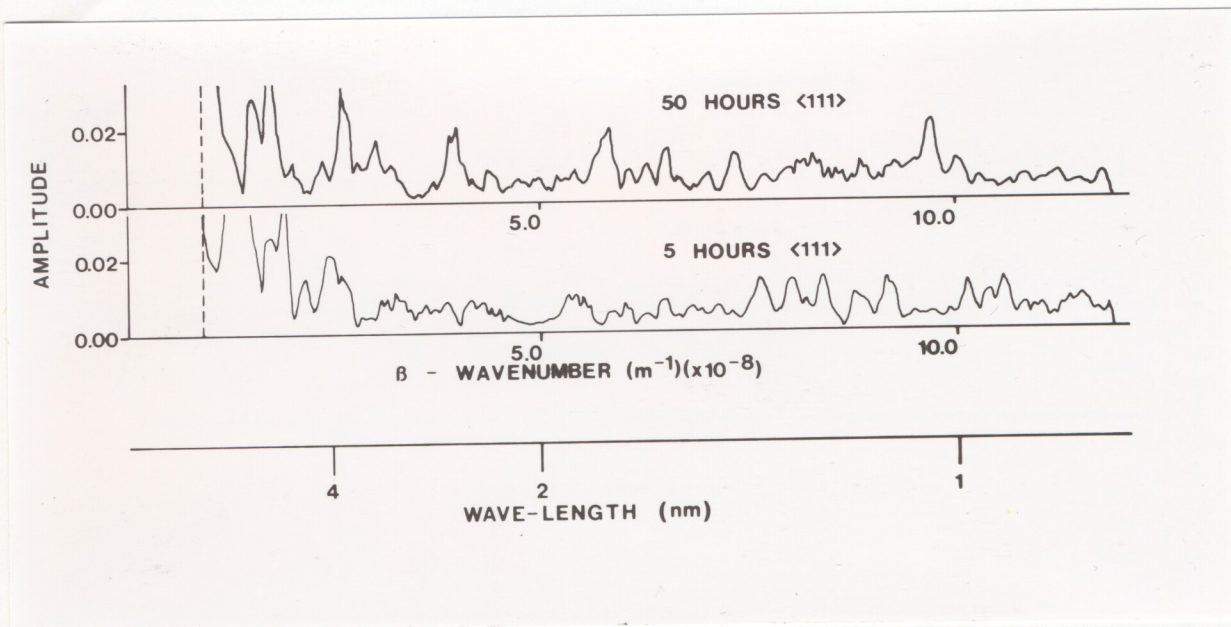


Figure 3.8 Net Fourier transforms for the two optimized simple grouping profiles of figure 3.6.



an approximately noiseless background the variance will tend to become stationary when dominant terms are successively removed from the amplitude data and  $V$  recalculated. Two criteria must be defined for this calculation of background variance: i) the amplitude deviation which is considered significant and ii) the maximum number of data values which should be removed. For the first, a departure of  $3\sigma$  from the current mean may be proposed. The second criterion essentially defines the acceptable degree of merging between dominant peaks and background. Studies showed that acceptable resolution is obtained where less than 20% of the initial data values are rejected before stationary variance was achieved.

#### 3.4.4 Comparison with Kinetic Theory

Kinetic equations for clustering have already been presented in Chapter 2 above. As a summary the following constructions are required in testing the character of transformation. 1) A plot of  $A_I(\beta)$  against time,  $t$ , for dominant wavenumbers. 2) A plot of the amplification factor,  $R(\beta)$ , (given by the slope of  $A_I(\beta)$  versus time) against  $\beta$ , and 3) Examination of  $R(\beta)/\beta^2$  versus  $\beta^2$ .

#### 3.5 Practical Analyses

Two net Fourier transforms obtained using the method outlined above are shown in figure 3.8. These are derived from the composition profiles shown in figures 3.6a and 3.6b. Each contains some dominant periodicities and several very dominant peaks (e.g.  $\beta = 2.50$  and  $\beta = 1.85 \times 10^3$ ) are common, increasing in amplitude as ageing increases. In each case background variance was found to be acceptable and stationary. For example, at  $\beta = 3.50$ ,  $V = 0.001$ .



Calculation of these transforms employed routine CO6AAF from the Nottingham Algorithm Group Library of the University of Cambridge Computing Service (Cooley-Tukey algorithm).

These calculations concerning Ni-14.1at.%Al have been extended also to tests of the diffusion equation predictions of Chapter 2. The results of the study, which demonstrated that decomposition is indeed continuous, form the basis of Chapter 4.

### 3.6 Assessment of the Fourier Method and Possible Extensions of Analysis.

#### 3.6.1 Sources of Error

Apart from errors involved in transform this method may be subject to inaccuracy associated with the original time series. For example:

- i) although specimens evaporate in an approximate plane-by-plane sequence individual events may be recorded from planes not immediately on the surface;
- ii) the series can take no account of changes of phase in oscillation accorded by antiphase domain boundaries in ordered structures;
- iii) similarly, grain boundaries and other defects are not considered.

However, the latter two effects may be detected by parallel observations of step profiles and overall it is considered that the time series analysis represents a reasonable approximation to true



behaviour. *to other experimental data*

### 3.6.2 Extensions of the Study

In principle the transform may simply be extended to encompass order-disorder composition modulations by retention of superlattice modulations and subtraction of all Fourier terms greater in wavelength than a few lattice periodicities. Similar Fourier techniques may also be applied to studies of plane stability ratio measurements (Sinclair, Ralph and Leake 1973) which are one of the more usual ways of studying order-disorder kinetics e.g. Taunt and Ralph 1974. *conditions other than*

*phase separation are discussed*

For small particle sizes studies of coarsening may also be envisaged.

In the course of the development of this method of Fourier analysis transforms corresponding to square-wave profiles of particles generated by conventional nucleation have been studied in addition to the modulated profiles of continuous phase separation. Since it has been shown that continuous transformations may be distinguished from nucleating systems (see Chapter 4 below), it may be envisaged that "idealized" transforms may be used for comparison with experimental composition data and transforms in order to provide a guide to the possible mode of phase separation. Some studies of this nature have been made by Biehl 1979; Piller 1979; Biehl and Wagner 1980.

It may also be noted that, although developed for use with atom-probe data, the proposed Fourier transform method may be applied in



principle to other experimental data chains.

### 3.7 Summary

This chapter has shown that data chains taken from atom-probe analyses are suitable for Fourier analysis. A composition profile which meets transform requirements has been developed. The chapter then outlines a sequence of steps in analysis designed to permit direct comparison of atom probe results with Fourier formulations of continuous transformation theories. Examples of transform results are given. Possible extensions of this analysis to transitions other than phase separation are discussed.